Structure and Reactions of ^{11}Be: Many-Body Basis for Single-Neutron Halo

F. Barranco,[1] G. Potel,[2] R. A. Broglia,[3,4] and E. Vigezzi[5]

[1]*Departamento de Fìsica Aplicada III, Escuela Superior de Ingenieros, Universidad de Sevilla,*
Camino de los Descubrimientos, 41092 Sevilla, Spain
[2]*National Superconducting Cyclotron Laboratory, Michigan State University, East Lansing, Michigan 48824, USA*
[3]*The Niels Bohr Institute, University of Copenhagen, DK-2100 Copenhagen, Denmark*
[4]*Dipartimento di Fisica, Università degli Studi Milano, Via Celoria 16, I-20133 Milano, Italy*
[5]*INFN Sezione di Milano, Via Celoria 16, I-20133 Milano, Italy*

The exotic nucleus ^{11}Be has been extensively studied and much experimental information is available on the structure of this system. We treat, within the framework of renormalized nuclear field theory in both configuration and 3D space, the mixing of bound and continuum single-particle states through the coupling to collective vibrations of the ^{10}Be core. We also take care of the Pauli principle acting not only between the single valence particle explicitly considered and those participating in the collective states, but also between fermions involved in two-phonon virtual states dressing the single-particle motion. In this way, it is possible to simultaneously and quantitatively account for the energies of the $1/2^+$, $1/2^-$ low-lying states, the centroid and line shape of the $5/2^+$ resonance and the one-nucleon stripping and pickup absolute differential cross sections involving ^{11}Be as either target or residual nucleus. Also for the dipole transition connecting the $1/2^+$ and $1/2^-$ parity inverted levels as well as the isotopic shift of the charge radius. Theory provides a unified and exhaustive nuclear structure and reaction characterization of the many-body effects which are at the basis of this paradigmatic one-neutron halo system.

If neutrons are progressively added to a light normal nucleus the Pauli principle forces, when the core becomes saturated, the wave functions of the last neutrons to move out and form a misty halo cloud. The resulting system displays a radius much larger than predicted by systematics, a sequence of levels contradicting the regular shell structure, and low-energy dipole transitions of strength ranked among the largest ever observed. The description of light exotic neutron-rich nuclei constitutes a formidable test of the ability of theory to simultaneously and on par account for (time dependent) mean field and many-body effects of similar magnitude, in which the nuclear surface and thus surface vibrations, play an overwhelming role.

The nucleus ^{11}Be constitutes one of the best and most studied—experimentally [1–8] and theoretically [9–25]—examples of the melting of the $N = 8$ closed shell, substituted by the new $N = 6$ magic number, a phenomenon resulting from the parity inversion between the $1p_{1/2}$, $2s_{1/2}$ levels. Less known, although not less important, is the conspicuous tendency to parity inversion, not fully materialized, displayed by the ($1p_{1/2}$, $d_{5/2}$) pair of levels.

Nuclear field theory (NFT), tailored after the Feynman diagrammatic version of quantum electrodynamics (QED), has been successfully employed to accurately describe, in many cases at the 10% or better error level, the nuclear structure of heavy (^{204}Pb [26], ^{209}Bi [27,28], ^{211}Pb [29], ^{212}At [30]), medium heavy ($^{118–122}$Sn [31–33]), and light two-neutron halo nuclei (^{11}Li [34], ^{12}Be [13]) with

predictions, also in this case, accurately confirmed by experiment [35,36]. After four decades of systematic application and development of NFT [37–39], we take up, in the present Letter, the challenge of describing the structure of ^{11}Be and the transfer reactions involving this nucleus, and attempt at answering central questions regarding its exotic properties: (i) Does it exist and if so, which is the mean field leading to the bare single-particle elementary modes of excitations which upon being dressed by vibrations, leads to the observed sequence of levels? (ii) Is there a universal mechanism at the basis of parity inversion and in the affirmative, has it been observed in other physical systems than the atomic nucleus? (iii) Which is the role played by many-body effects involving continuum states, regarding both resonances and single-particle transfer processes?

In the calculations discussed in this Letter, we have simultaneously dealt with the $p_{3/2}$, $p_{1/2}$, $s_{1/2}$, and $d_{5/2}$ single-particle states up to an energy $E_{cut} = 25$ MeV, imposing vanishing boundary conditions at $R = 50$ fm (continuum discretization), treating their interweaving with the quadrupole collective vibrations of the ^{10}Be core (Supplemental Material, Sec. 2 [40]) and taking into account the mixing between bound and continuum states. The same calculations have been repeated including also the octupole and the pair removal modes of the core ^{10}Be (see Supplemental Material, Secs. 2 and 3 [40] and Ref. [41]), obtaining very similar results, and no physical effect not already found within the quadrupole vibration

subspace (in connection with the simultaneous treatment of particle-hole and pairing vibrations, see also Refs. [42,43]).

There are in all four parameters entering the calculations discussed in this Letter [the depth V, the radius R, the diffusivity a, and the spin-orbit strength V_{ls}, see Ref. [44], Eq. (2–180)] which are allowed to vary freely in an attempt to determine the bare potential making use of an effective mass [$m_k = 0.7m(0.91m)$ for $r = 0$ ($r = \infty$); see Supplemental Material, Sec. 1 [40]], and three experimental (empirical) inputs, namely, the excitation energy $\hbar\omega_2$ ($= 3.368$ MeV) and the dynamical deformation $\beta_2^n(\approx 0.9)$, which characterize the low-lying quadrupole vibration of the core $^{10}_4\text{Be}_6$, together with the electromagnetic deformation parameter $\beta_2^{em} = 1.13$ (see Supplemental Material, Sec. 2 [40] and Refs. [1,45,46]). The large value of β_2^n underscores the fact that the system is close to a quadrupole shape phase transition, a phenomenon closely connected with α clustering in a light nucleus like ^{10}Be.

Because of spatial quantization, the above scheme involves both energies and single-particle radial wave functions, in particular those associated with the $d_{5/2}$ resonance. The variety of many-body clothing processes leads to important modifications of these radial wave functions, and thus of the corresponding one-particle transfer form factors and escape particle wave functions, accounting for up to 50% changes in the value of the one-nucleon transfer absolute cross sections and of the $5/2^+$ resonance decay width, in overall agreement with experimental data. Important information concerning the nature of the $5/2^+$ resonance, and of the role the quadrupole mode plays in dressing the nucleons moving around the Fermi surface is provided by the reactions $^{10}\text{Be}(d, p)^{11}\text{Be}(5/2^+, 1.783 \text{ MeV})$ and $^{11}\text{Be}(p, d)^{10}\text{Be}(2^+; 3.368 \text{ MeV})$, which forces, in this last case, a virtual state to become observable. A fact that aside from shedding light on retardation mechanisms in clothing processes, implies that particle-vibration coupled intermediate states which dress the single-particle states have to be real states concerning both energy and amplitude, as well as radial shape. Thus, $(\text{NFT})_{\text{ren}}$ (Ref. [39] and references therein, see also Refs. [33,37,47]) is not a calculational ansatz but a quantal requirement. Within this context, it is of notice that self-consistency within $(\text{NFT})_{\text{ren}}$ implies that the renormalized $\tilde{\epsilon}_j$ and $\tilde{\phi}_j(r)^{(i)}$ quantities reproduce the empirical input used for the intermediate states, while initial states (energies and wave functions) of the different graphical contributions are solutions of the bare potential (Fig. 1). In other words, for each value of $\tilde{\epsilon}_j$ there can exist more than one radial function, depending on whether the nucleon is moving around the ground state ($i = gs$) or around an excited collective state ($i = \lambda^\pi$) of the core, respectively (see Supplemental Material, Sec. 9 [40]). Technically, $\tilde{\phi}_j(r)^{(i)}$ are the form factors associated with stripping and pickup reactions around closed shells. For simplicity we will drop the superscript i in what follows.

Making use of the $(\text{NFT})_{\text{ren}}$ framework we have calculated the variety of self-energy diagrams, renormalizing
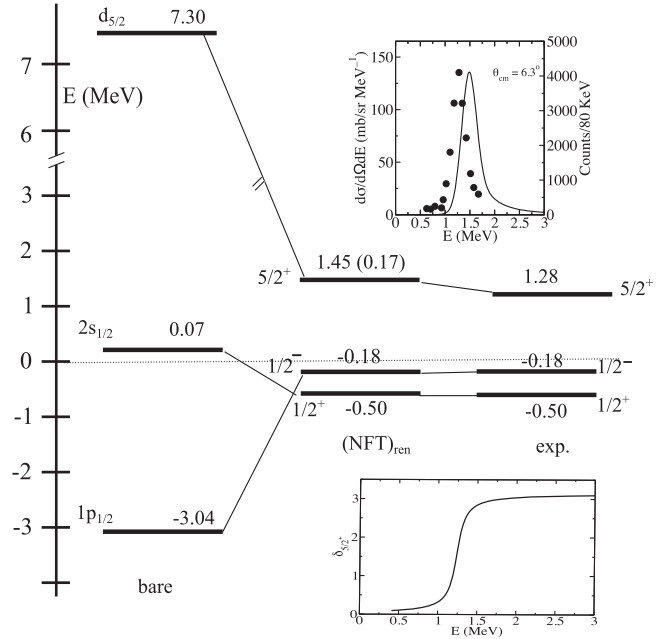

FIG. 1. Low-lying spectrum of ^{11}Be: (bare) unperturbed single-particle levels, solution of the bare mean field (see Supplemental Material, Sec. 1 [40]); [$(\text{NFT})_{\text{ren}}$] dressed levels; (exp.) experimental values. The number on each thick horizontal line gives the energy of the state in MeV. The number in brackets corresponds to the width of the $5/2^+$ resonance derived from the calculated elastic phase shifts (see inset on the lower rhs). No phase shift data exist for this state, the 100 keV width often quoted being extracted from the $^9\text{Be}(t, p)^{11}\text{Be}(5/2^+)$ reaction (Ref. [48], Table 11.5). The line shape of the $5/2^+$ resonance calculated from the $(d^2\sigma/d\theta dE)_{\theta=6.3^o}$ $[^{10}\text{Be} \rightarrow ^{11}\text{Be}(5/2^+)]$ strength function (see Supplemental Material, Sec. 10 [40]) is displayed in the upper rhs corner inset (continuous line) in comparison with the data (solid dots) [6].

self-consistently the motion of the odd neutron of ^{11}Be in both configuration (Fig. 2) and conformational 3D space (Fig. 3), through the coupling to quadrupole vibrations. The dressed states associated with a given quantum number result from the iterative diagonalization of the particle-vibration coupling (PVC) Hamiltonian in a space composed of single-particle and of particle-phonon states, making use of self-energy function techniques [Fig. 2(I), see also Supplemental Material, Sec. 4 [40]]. The resulting states can be written as

$$|\widetilde{1/2^+}\rangle = \sqrt{0.80}|s_{1/2}\rangle + \sqrt{0.20}|(d_{5/2} \otimes 2^+)_{1/2^+}\rangle, \quad (1)$$

$$|\widetilde{1/2^-}\rangle = \sqrt{0.84}|p_{1/2}\rangle$$
$$+ \sqrt{0.16}|(p_{1/2}, p_{3/2}^{-1})_{2^+} \otimes 2^+)_{0^+}, p_{1/2}\rangle, \quad (2)$$

$$|\widetilde{5/2^+}\rangle = \sqrt{0.49}|d_{5/2}\rangle + \sqrt{0.23}|(s_{1/2} \otimes 2^+)_{5/2^+}\rangle$$
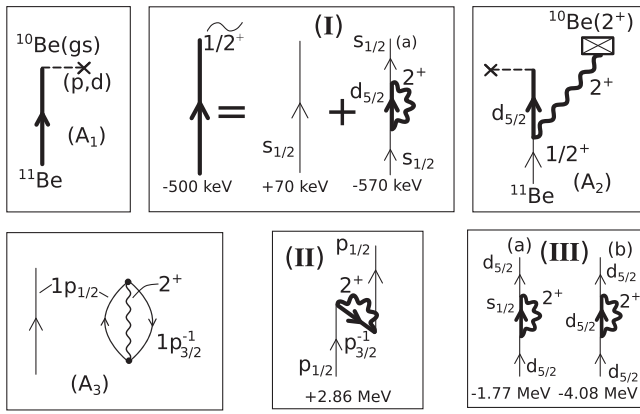$$+ \sqrt{0.28}|(d_{5/2} \otimes 2^+)_{5/2^+}\rangle. \quad (3)$$

FIG. 2. $(\text{NFT})_{\text{ren}}$ diagrams describing the renormalization processes responsible for the different components of the clothed states [Eqs. (1)–(3) associated with (I)–(III)] and the pickup processes populating the ground (A_1) and the first excited 2^+ state (A_2) of ^{10}Be. (A_3) Valence nucleon in the presence of a virtual zero point fluctuation of the core ^{10}Be. Bold (thin) arrowed lines pointing upwards (downwards), describe dressed (bare) particle (hole) states. The wavy line represents the quadrupole vibration. A cross followed by a horizontal dashed line stands for an external one-neutron pickup (p, d) field. A crossed box indicates a detector, revealing the γ ray associated with the eventual decay of the quadrupole vibration of ^{10}Be.

The bare energies ϵ_j and the values $[(\text{NFT})_{\text{ren}}]\ \tilde{\epsilon}_j$ associated with the renormalized single-particle states are shown in Fig. 1 in comparison with the experimental data. The corresponding wave functions $\phi_j(r)$ and $\tilde{\phi}_j(r)$ are displayed in Fig. 3. Concerning the bare potential leading to ϵ_j and $\phi_j(r)$, we refer to the Supplemental Material, Sec. 1 [40]. As seen from Fig. S1 there, the bare states are essentially equal to the HF solution of the SGII-Skyrme interaction. The most conspicuous effect emerging from NFT results is the reduction (in absolute value) of the energy difference between the positive and negative parity states (Fig. 1): a factor of 10 in the case of the $1/2^-$, $1/2^+$ states and of six in the case of the $5/2^+$, $1/2^-$ states. While parity inversion is only observed in the first case, the second had a close call.

Let us start by discussing the properties of the $\widetilde{5/2^+}$ resonance. This state is prone to acquire a dynamical

quadrupole moment (reorientation effect). This is because the particle-vibration coupling of the $d_{5/2^+}$ with itself [Fig. 2(III)(b)] through the excitation of the quadrupole vibration of ^{10}Be, involves a rather confined single-particle resonant state radial wave function [Fig. 3(c)]. It results in a large (absolute) value of the associated PVC matrix element leading to an amplitude of $\sqrt{0.28}$ for the many-body component $|(d_{5/2} \otimes 2^+)_{5/2^+}\rangle$ of the $|\widetilde{5/2^+}\rangle$ state [Eq. (3)]. An equally important component ($\approx\sqrt{0.23}$) is associated with the coupling of the $5/2^+$ state to the $s_{1/2}$ state, again through the quadrupole mode [Fig. 2(III)(a)]. This coupling allows the bare $d_{5/2}$ resonance ($\epsilon_{5/2^+} \approx$ 7.3 MeV, Fig. 1), to explore halolike regions of the system and to lower its kinetic energy. Overall, these couplings result in an energy decrease of the $5/2^+$ strength and in the buildup of a narrow resonance with centroid at $E =$ 1.45 MeV and a width of 170 keV as calculated from elastic scattering phase shifts (see lower left-hand side inset, Fig. 1 and Supplemental Material, Sec. 4 [40]). In turn, the $2s_{1/2}$ wave function mixes with the $(d_{5/2} \otimes 2^+)$ configuration and acquires a component of sizable amplitude [$\approx\sqrt{0.20}$, Eq. (1)] lowering, in the process, its bare energy by about 570 keV [Fig. 2(I)(a)] and getting bound by 0.5 MeV. In other words, the $d_{5/2}$ state plays, through its coupling to the 2^+ vibration of the core, an essential role in the $(1/2^-, 1/2^+)$ parity inversion phenomenon, by lowering the energy of the $s_{1/2}$ state conspicuously. The numbers quoted above also contain the renormalization contribution of the Pauli correcting diagrams associated with the implicit presence of two-phonon states in intermediate, virtual configurations [49]. Otherwise, the corrections arising from the self-energy processes shown in Fig. 2(I) and 2(III) would have been much too attractive (see Supplemental Material, Sec. 6 [40]).

The zero-point fluctuations associated with the ^{10}Be core, arising from the quadrupole vibrations [Fig. 2(A_3)], make virtual use of the $p_{1/2}$ single-particle state. The diagram displayed in Fig. 2(II) properly treats this problem, namely, the antisymmetry between the valence nucleon and those participating in the vibration. As a result, the phase space of the clothed $\widetilde{1/2^-}$ state becomes smaller than the
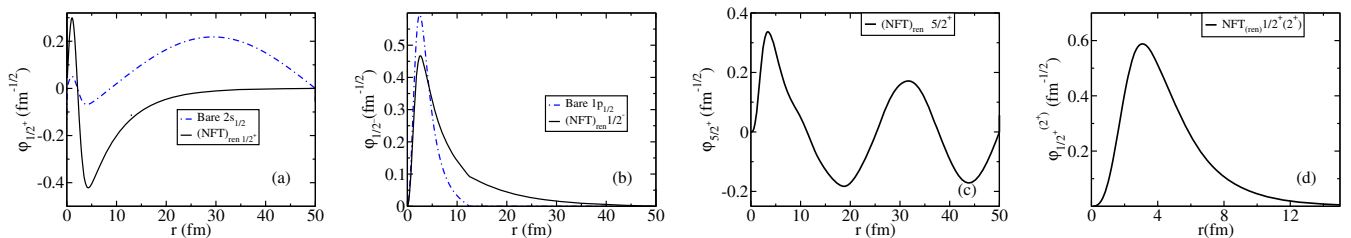

FIG. 3. Form factors of the $\widetilde{1/2^+}$ (a), $\widetilde{1/2^-}$ (b), $\widetilde{5/2^+}$ (c) states and (d) the form factor associated with the reaction ^{11}Be$(p, d)^{10}$Be(2^+) calculated within the framework of $(\text{NFT})_{\text{ren}}$ [$a_{1/2^+} = \sqrt{0.80}, a_{1/2^-} = \sqrt{0.84}, a_{5/2^+} = \sqrt{0.49}, a_{(d_{5/2}\otimes 2^+)_{1/2^+}} = \sqrt{0.20}$, see Eqs. (1)–(3)]. Also shown in (a) and (b) are the wave functions calculated with the bare potential (see also Supplemental Material, Sec. 9 [40]).

bare one, its binding becoming weaker by about 3 MeV due to a rather conspicuous Lamb-shift-like effect, of the order of 10% of the value of the Fermi energy. Over counting (bubble corrections) is, in the present case, negligible (see Supplemental Material, Sec. 5 [40]).

The radial dependence of the many-body wave functions and the phonon admixture in single-neutron states can be probed by the one-neutron transfer reactions $^{10}\text{Be}(d, p)^{11}\text{Be}$ and $^{11}\text{Be}(p, d)^{10}\text{Be}(2^+)$, populating the low-lying $1/2^+$, $1/2^-$, and $5/2^+$ states of ^{11}Be and the first excited 2^+ state of ^{10}Be, and proceeding through the form factors displayed in Figs. 3(a)–3(c) and Fig. 3(d), respectively. Concerning the latter, we remark that the asymptotic decay constant of the $d_{5/2}$ radial wave function $\tilde{\phi}_{1/2^+}(r)^{(2^+)}$ associated with the $2^+ \otimes d_{5/2}$ configuration admixed in the $1/2^+$ ground state of ^{11}Be displays a binding energy $\tilde{\epsilon}_{1/2^+} - \hbar\omega_{2^+} = -3.8$ MeV. This is a natural outcome of $(\text{NFT})_{\text{ren}}$ which, through PVC and the Pauli mechanism, provides the proper clothing of the $d_{5/2}$ orbital so as to make it able "to exist" inside the $|\widetilde{1/2^+}\rangle$ state as a virtual, intermediate configuration [Fig. 2(I)(a)]. The associated asymptotic r behavior results from the coherent superposition of many continuum states, and its spatial dependence in the surface region [Fig. 3(d)] can hardly be simulated by making use of a bound single-particle wave function of a properly parametrized single-particle potential (separation energy approximation, commonly used in the literature), an outcome which is in agreement with the result of previous studies [3].

The $(\text{NFT})_{\text{ren}}$ form factors shown in Fig. 3 were used, together with global optical potentials [50,51], to calculate the one-nucleon stripping and pickup absolute differential cross sections of the reactions mentioned above (see Supplemental Material [40], Sec. 10). The results provide an overall account of the experimental findings (Fig. 4). Within this context we remark that the pickup process shown in inset (A_1) of Fig. 2 populating the ^{10}Be ground state implies the action of the external (p, d) field on the left-hand side (lhs) of the graphical representation of the Dyson equation shown in Fig, 2(I), and involves, at the same time, the use of the corresponding radial wave

function as a form factor [Fig. 3(a)]. In the case of the population of the first 2^+ excited state of ^{10}Be (inset A_2), the (p, d) field acts on the $(d_{5/2} \otimes 2^+)_{1/2^+}$ virtual state of the second graph of the right-hand side (rhs) of this equation [Fig. 2(I)(a)], involving this time the radial wave function $\tilde{\phi}_{1/2^+}(r)^{(2^+)}$ as the form factor [Fig. 3(d)]. Summing up, insets (A_1) and (A_2) and diagrams (I) of Fig. 2 testify to the subtle effects resulting from the unification of $(\text{NFT})_{\text{ren}}$ of structure and reactions discussed in Ref. [39], and operative in the cross sections shown in Fig. 4, as a result of the simultaneous and self-consistent treatment of configuration and 3D space. Within this context the bold face drawn state $|(d_{5/2} \otimes 2^+)_{1/2^+}\rangle$ shown in Fig. 2(I)(a) and the radial wave function $(\text{NFT})_{\text{ren}}$ displayed in Fig. 3(d) can be viewed as an on par structure and reaction intermediate elements of the quantal process $^{11}\text{Be}(p, d)^{10}\text{Be}(2^+)$.

PVC leads also to important renormalization effects in the dipole electromagnetic transitions of the system. This is due to the poor overlap between the renormalized halo radial wave functions and those of the core nucleons which screen the symmetry potential, impeding the GDR to shift the $1/2^+ \rightarrow 1/2^-$ single-particle E1 strength to high energies in an attempt to exhaust the EWSR [52]. The strength of the dipole transition calculated making use of the dressed states leads to $B(E1; 1/2^- \rightarrow 1/2^+) = 0.11\ e^2\ \text{fm}^2$, a value to be compared to the experimental value $B(E1) = 0.102 \pm 0.002\ e^2\ \text{fm}^2$ [8]. No free parameters were used in the calculations (for details see Supplemental Material, Sec. 7 [40]).

We now discuss the isotopic shift of the charge radius (Supplemental Material, Sec. 8 [40]). The corrections to $\langle r^2 \rangle^{1/2}_{^{10}\text{Be}}$ arising from the addition of a neutron are obtained applying the external field operator r^2 to the different particle and collective vibration lines of the diagrams appearing on the rhs of the graphical equation displayed in Fig. 2(I). The summed (recoil) contributions associated with the $s_{1/2}$ state $(\langle r^2 \rangle^{1/2}_{1/2^+}/11)^2 (\langle r^2 \rangle^{1/2}_{1/2^+} = 7.1\ \text{fm})$ are to be multiplied by the square of the renormalized $|\widetilde{1/2^+}\rangle$ state single-particle amplitude [$= 0.80$, Eq. (1)]. Those
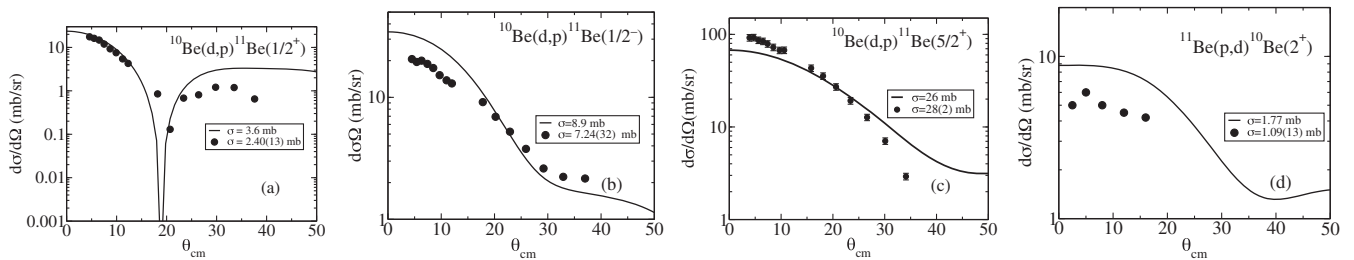

FIG. 4. (a)–(c) (continuous curve) Absolute differential and (insets) summed cross sections associated with the reactions $^2\text{H}(^{10}\text{Be}, ^{11}\text{Be})^1\text{H}$ at $E = 107$ MeV, populating the $1/2^+$, $1/2^-$, and $5/2^+$ states. The experimental data [6] are displayed in terms of solid dots. (d) Same as before, but for the reaction $^1\text{H}(^{11}\text{Be}, ^{10}\text{Be})^2\text{H}$ at $E = 388.3$ MeV, populating the 2^+ state [3].

associated with the $d_{5/2}$ and 2^+ elementary modes appearing in the intermediate state of graph (a) of Fig. 2(I) lead to (recoil) $(\langle r^2 \rangle^{1/2}_{(d_{5/2} \otimes 2^+)_{1/2^+}} / 11)^2$ and (dynamical deformation) $(((\langle r^2 \rangle_{^{10}Be}(\beta_2^{em})^2)^2 / 2\pi)$ contributions, respectively, and are to be multiplied by the square amplitude ($= 0.20$) associated with the $(d_{5/2} \otimes 2^+)_{1/2^+}$ configuration [Eq. (1)]. The resulting theoretical prediction $\langle r^2 \rangle^{1/2}_{^{11}Be} = 2.48$ fm, accurately reproduces the experimental finding 2.466 ± 0.015 fm [19].

We conclude that the existence of a bare potential and associated k mass whose eigenstates essentially coincide with the HF solution of the SGII Skyrme interaction, forcefully testifies to the validity of mean-field approaches in the description of light halo nuclei in general, and ^{11}Be in particular. The fact that a substantial fraction of the low-lying single-particle states, as much as 50% in the case of the $d_{5/2}$ state, corresponds to many-body configurations as well as the strong Pauli principle repulsion associated with two-quadrupole phonon virtual states dressing single-particle motion, testifies equally forcefully to the time-dependent nature of the mean field, let alone the strong anharmonic character of this dependence.

Parity inversion results mainly from Pauli blocking of the ground state (quadrupole) zero-point fluctuations of the core ^{10}Be by the odd $p_{1/2}$ neutron, together with the dressing of the $s_{1/2}$ state by the same vibration. The physics at the basis of this phenomenon has been observed for the first time in the spectrum of hydrogen atoms by Lamb and co-workers [53,54]. The Lamb shift, that is the fact that the $2s_{1/2}$ level of H lies higher than the $2p_{1/2}$ by 1058 MHz (4.4 μeV), while Dirac equation predicts them to be degenerate, provided the first measure of QED vacuum fluctuations. Within the context of nuclear physics, one can mention that the relatively "large" upshift ($+129$ keV) of the $I = 15/2^+$ member of the $[h_{9/2}(\pi) \otimes 3^- (^{208}Pb)]_I$ septuplet of ^{209}Bi, one of the first experimental tests to which NFT was subject, has the same origin as the 2860 keV upshift of the $p_{1/2}$ level of ^{11}Be.

At the basis of the large magnitude of the renormalization effects observed in ^{11}Be, one finds a fundamental parameter of NFT, namely, the effective degeneracy $\Omega(\approx 2/3 A^{2/3})$ of the single-particle phase space, $1/\Omega$ being the small expansion parameter. In the case of ^{11}Be, Ω is rather small (≈ 3) as compared with heavy nuclei like, e.g., ^{209}Bi ($\Omega \approx 24$), a fact that underscores the need to sum to all orders (in $1/\Omega$) those processes operative in the dressing of single-particle states. Furthermore, in the case of ^{11}Be, the surface (S) to volume (V) ratio ($r = aS/V$, a being the diffusivity) is much larger (≈ 0.74) than in the case of heavy nuclei lying along the stability valley (≈ 0.28 in the case of ^{209}Bi).

Finally, one can posit that the renormalization of the radial dependence of the single-particle states due to the many-body processes involving the continuum states plays an important role in the absolute one-nucleon transfer differential cross sections.

[1] H. Iwasaki *et al.*, Phys. Lett. B **481**, 7 (2000).
[2] S. Fortier *et al.*, Phys. Lett. B **461**, 22 (1999).
[3] J. S. Winfield *et al.*, Nucl. Phys. **A683**, 48 (2001).
[4] D. L. Auton, Nucl. Phys. **A157**, 305 (1970).
[5] B. Zwieglinski, W. Benenson, R. G. H. Robertson, and W. R. Coker, Nucl. Phys. **A315**, 124 (1979).
[6] K. T. Schmitt *et al.*, Phys. Rev. C **88**, 064612 (2013).
[7] W. Nörtershäuser *et al.*, Phys. Rev. Lett. **102**, 062503 (2009).
[8] E. Kwan *et al.*, Phys. Lett. B **732**, 210 (2014).
[9] I. Talmi and I. Unna, Phys. Rev. Lett. **4**, 469 (1960).
[10] T. Otsuka, N. Fukunishi, and H. Sagawa, Phys. Rev. Lett. **70**, 1385 (1993).
[11] H. Sagawa, B. A. Brown, and H. Esbensen, Phys. Lett. B **309**, 1 (1993).
[12] N. Vinh Mau, Nucl. Phys. **A592**, 33 (1995).
[13] G. Gori, F. Barranco, E. Vigezzi, and R. A. Broglia, Phys. Rev. C **69**, 041302(R) (2004).
[14] F. M. Nunes, I. J. Thompson, and R. C. Johnson, Nucl. Phys. **A596**, 171 (1996).
[15] K. Fossez, W. Nazarewicz, Y. Jaganathen, N. Michel, and M. Ploszajczak, Phys. Rev. C **93**, 011305(R) (2016).
[16] I. Hamamoto and S. Shimoura, J. Phys. G **34**, 2715 (2007).
[17] Y. Kanada-En'yo and H. Horiuchi, Phys. Rev. C **66**, 024305 (2002).
[18] A. Calci, P. Navrátil, R. Roth, J. Dohet-Eraly, S. Quaglioni, and G. Hupin, Phys. Rev. Lett. **117**, 242501 (2016).
[19] A. Krieger *et al.*, Phys. Rev. Lett. **108**, 142501 (2012).
[20] N. K. Timofeyuk and R. C. Johnson, Phys. Rev. C **59**, 1545 (1999).
[21] N. Keeley, N. Alamanos, and V. Lapoux, Phys. Rev. C **69**, 064604 (2004).
[22] A. Deltuva, Phys. Rev. C **79**, 054603 (2009).
[23] A. Deltuva, Phys. Rev. C **88**, 011601(R) (2013).
[24] J. A. Lay, A. M. Moro, J. M. Arias, and Y. Kanada-En'yo, Phys. Rev. C **89**, 014333 (2014).
[25] R. de Diego, J. M. Arias, J. A. Lay, and A. M. Moro, Phys. Rev. C **89**, 064609 (2014).
[26] P. F. Bortignon, R. A. Broglia, and D. R. Bes, Phys. Lett. B **76**, 153 (1978).
[27] P. F. Bortignon *et al.*, Phys. Rep. **30**, 305 (1977).
[28] A. Bohr and B. R. Mottelson, *Nuclear Structure* (Benjamin, New York, 1975), Vol. II.
[29] O. Civitarese, R. A. Broglia, and D. R. Bes, Phys. Lett. B **72**, 45 (1977).
[30] F. A. Janouch, and R. J. Liotta, Phys. Lett. B **82**, 329 (1979).
[31] A. Idini, Ph.D. thesis, University of Milano, unpublished.
[32] A. Idini, F. Barranco, and E. Vigezzi, Phys. Rev. C **85**, 014331 (2012).

[33] A. Idini, G. Potel, F. Barranco, E. Vigezzi, and R. A. Broglia, Phys. Rev. C **92**, 031304(R) (2015).

[34] F. Barranco, P. F. Bortignon, R. A. Broglia, G. Colò, and E. Vigezzi, Eur. Phys. J. A **11**, 385 (2001).

[35] I. Tanihata et al., Phys. Rev. Lett. **100**, 192502 (2008).

[36] G. Potel, F. Barranco, E. Vigezzi, and R. A. Broglia, Phys. Rev. Lett. **105**, 172502 (2010).

[37] D. R. Bes, G. G. Dussel, R. P. J. Perazzo, and H. M. Sofía, Nucl. Phys. **A293**, 350 (1977).

[38] D. R. Bes and J. Kurchan, *The Treatment of Collective Coordinates in Many-Body Systems* (World Scientific, Singapore, 1990).

[39] R. A. Broglia, P. F. Bortignon, F. Barranco, E. Vigezzi, A. Idini, and G. Potel, Phys. Scr. **91**, 063012 (2016).

[40] See Supplemental Material at http://link.aps.org/supplemental/10.1103/PhysRevLett.119.082501 for details of the results of the calculations which are at the basis of the present Letter as well as of those obtained including also the pair removal and octupole modes of ^{10}Be, which are mentioned in the text.

[41] G. Blanchon, N. V. Mau, A. Bonaccorso, M. Dupuis, and N. Pillet, Phys. Rev. C **82**, 034313 (2010).

[42] W. H. Dickhoff and D. Van Neck, *Many-Body Theory Exposed!: Propagator Description of Quantum Mechanics in Many-Body Systems* (World Scientific, Singapore, 2008).

[43] C. Barbieri and W. H. Dickhoff, Phys. Rev. C **68**, 014311 (2003).

[44] A. Bohr and B. R. Mottelson, *Nuclear Structure* (Benjamin, New York, 1969), Vol. I.

[45] S. Raman, C. H. Malarkey, W. T. Milner, C. W. Nestor, and P. H. Stelson, At. Data Nucl. Data Tables **36**, 1 (1987).

[46] A. M. Bernstein, V. R. Brown, and V. A. Madsen, Phys. Lett. B **103**, 255 (1981).

[47] R. D. Mattuck, *A Guide to Feynman Diagrams in the Many-Body Problem* (Dover, New York, 1976).

[48] J. H. Kelley, E. Kwan, J. E. Purcell, C. G. Sheu, and H. R. Weller, Nucl. Phys. **A880**, 88 (2012).

[49] D. R. Bès, R. A. Broglia, G. G. Dussel, R. J. Liotta, and H. M. Sofia, Nucl. Phys. **A260**, 1 (1976).

[50] Y. Han, Y. Shi, and Q. Shen, Phys. Rev. C **74**, 044615 (2006).

[51] J. Koning and J.-P. Delaroche, Nucl. Phys. **A713**, 231 (2003).

[52] P. F. Bortignon, A. Bracco, and R. A. Broglia, *Giant Resonances* (Harwood Academic Publishers, Amsterdam, 1998).

[53] W. Lamb and R. Retherford, Phys. Rev. **72**, 241 (1947).

[54] N. M. Kroll and W. E. Lamb, Phys. Rev. **75**, 388 (1949).